METFORMIN LOWERS PLASMA TRIGLYCERIDES BY PROMOTING VLDL-TRIGLYCERIDE CLEARANCE BY BROWN ADIPOSE TISSUE IN MICE

7

Janine J. Geerling
Mariëtte R. Boon
Gerard C. van der Zon
Sjoerd A.A. van den Berg
Anita M. van den Hoek
Hans M.G. Princen
Louis M. Havekes
Patrick C.N. Rensen
Bruno Guigas

Submitted

ABSTRACT

Metformin is the first-line drug for the treatment of type 2 diabetes. Besides its well-characterized antihyperglycemic properties, metformin also lowers plasma very low-density lipoprotein (VLDL)-cholesterol and VLDL-triglycerides (TG). In this study, we investigated the underlying molecular mechanisms in APOE*3-Leiden.CETP mice, a well-established model for human-like lipoprotein metabolism. We found that metformin markedly lowered plasma total cholesterol and TG without affecting body weight, food intake and plasma levels of glucose, insulin and free fatty acids. Analysis of lipoprotein profiles revealed that metformin reduced plasma VLDL and slightly increased high-density lipoprotein levels. Metformin did not affect hepatic VLDL-TG production, VLDL particle composition and hepatic lipid composition. In contrast, metformin selectively enhanced clearance of glycerol tri[^{3}H]oleate-labeled VLDL-like emulsion particles into brown adipose tissue (BAT). At the molecular level, this was accompanied by higher AMPKα1 activity and increase in both hormone-sensitive lipase and mitochondrial content, suggesting that metformin enhances VLDL-TG uptake, intracellular TG lipolysis, and subsequent mitochondrial fatty acid oxidation in BAT. Collectively, our results identify BAT as an important player in the TG-lowering effect of metformin, suggesting that targeting this tissue might be of therapeutic interest in the treatment of dyslipidemia.

INTRODUCTION

Metformin is one of the most widely used glucose-lowering agents for the treatment of type 2 diabetes [1] and is now considered as the first-line drug therapy for patients [2]. This antidiabetic drug from the biguanides family is prescribed for its effective antihyperglycemic action, mostly achieved through a potent reduction of hepatic glucose production secondary to inhibition of gluconeogenesis [3]. Interestingly, another important but often overlooked property of metformin relies on its beneficial effect on blood lipid profile which is characterized by a significant reduction in circulating triglycerides (TG) and very low-density lipoprotein (VLDL) cholesterol, and increased high-density lipoprotein (HDL) cholesterol levels [4]. This metabolic feature might partly be involved in its cardio-protective effect observed in obese patients treated with the drug [5]. Despite extensive efforts during the last years [6], the exact molecular mechanism(s) of action of metformin still remain incompletely understood, especially the one by which the drug exerts its lipid-lowering action. In 2001, Zhou *et al.* were the first to report that metformin activates hepatic AMP-activated protein kinase (AMPK), emphasizing the putative role of this energy-sensing kinase in the mechanism of action of the drug [7].

AMPK is a well-conserved serine/threonine protein kinase that plays a crucial role in the regulation of catabolic/anabolic pathways by acting as a cellular energy and nutrient sensor [8, 9]. AMPK consists of a heterotrimeric complex containing a catalytic α subunit and two regulatory β and γ subunits. Each subunit has several isoforms (α1, α2; β1, β2; γ1, γ2, γ3), which are encoded by distinct genes, giving multiple heterotrimeric combinations with tissue-specific distribution [8, 9]. The α subunit contains a threonine residue (Thr 172) whose phosphorylation by upstream kinases, such as the liver kinase B (LKB1), is required for AMPK activation. The β subunit acts as a scaffold to which the two other subunits are bound, and also allows AMPK to sense energy reserves in the form of glycogen [8, 9]. Binding of AMP and/or ADP to selective domains on the γ subunit leads to AMPK activation via a complex mechanism involving direct allosteric activation, phosphorylation on Thr172 by AMPK upstream kinases and inhibition of dephosphorylation of this residue by specific protein phosphatases that remain to be identified [8, 9]. Thus, any decrease in cellular energy status activates AMPK, which results, through phosphorylation of various downstream targets, in concomitant inhibition of energy-consuming processes and stimulation of ATP-generating pathways in order to restore energy balance. Interestingly, the mechanism by which metformin activates AMPK, involving specific inhibition of the mitochondrial respiratory chain complex 1 [10, 11], was recently clarified [12, 13], although the contribution of the LKB1/AMPK axis in its hepatic effects still remains controversial [14–18].

The objective of this study was to investigate the molecular mechanisms underlying the effects of metformin on lipoprotein metabolism, by using APOE*3-Leiden. CETP (*E3L.CETP*) transgenic mice, a well-established model with a human-like

lipoprotein metabolism. Collectively, our data show that treatment of *E3L.CETP* mice with metformin is able to recapitulate the lipid-lowering effect of the drug evidenced in humans, *i.e* causing a reduction in plasma VLDL-TG associated with a parallel mild increase in HDL-cholesterol. Remarkably, this effect is not mediated by apparent changes in hepatic VLDL-TG production but rather by a selective increase in VLDL-TG clearance by the brown adipose tissue (BAT). At the molecular level, we found an increase in AMPKα1 activity and protein expression of both hormone-sensitive lipase (HSL) and mitochondrial respiratory-chain complexes, suggesting that metformin promotes intracellular TG lipolysis and subsequent mitochondrial fatty acid (FA) oxidation in BAT.

MATERIALS AND METHODS

Materials

All chemicals were purchased from Sigma-Aldrich (St. Louis, MO, USA).

Ethics

All mouse experiments were performed in accordance with the Institute for Laboratory Animal Research Guide for the Care and Use of Laboratory Animals and have received approval from the university Ethical Review Boards (Leiden University Medical Center, Leiden, The Netherlands).

Animals, diet, and metformin treatment

Homozygous human CETP transgenic mice were crossbred with hemizygous APOE*3-Leiden (*E3L*) mice at our Institutional Animal Facility to obtain *E3L.CETP* mice, as previously described [19]. In this study, 12 weeks-old *E3L.CETP* female mice, housed under standard conditions in conventional cages with *ad libitum* access to food and water, were fed a Western-type diet containing 0.1% (w/w) cholesterol (Hope Farms, Woerden, the Netherlands) for 4 weeks. Upon randomization according to body weight, plasma total cholesterol (TC) and triglyceride (TG) levels, mice next received a Western-type diet with or without 200 mg/kg BW/day (0.2%, w/w) metformin for 4 weeks. Unless otherwise mentioned, experiments were performed after 4 h of fasting at 13:00 pm with food withdrawn at 9:00 am.

Plasma lipid and lipoprotein analysis

Plasma was obtained via tail vein bleeding and assayed for TC, TG and PL using the commercially available enzymatic kits 236691, 11488872 and 1001140 (Roche Molecular Biochemicals, Indianapolis, IN, USA), respectively. Free fatty acids (FA) were measured using NEFA-C kit from Wako Diagnostics (Instruchemie, Delfzijl, the Netherlands). The distribution of lipids over plasma lipoprotein fractions was determined using fast protein liquid chromatography. Plasma was pooled per group, and 50 μl of each pool was injected onto a Superose 6 PC 3.2/30 column (Akta System, Amersham Pharmacia Biotech, Piscataway, NJ, USA) and eluted at a constant flow rate of 50 μl/min in 1mM EDTA in PBS, pH 7.4. Fractions of 50 μl were collected and assayed for TC and TG as described above.

Hepatic VLDL-TG and VLDL-apoB production

Mice were fasted for 4 h prior to the start of the experiment. During the experiment, mice were sedated with 6.25 mg/kg BW Acepromazine (Alfasan, Woerden, The Netherlands), 6.25 mg/kg BW Midazolam (Roche, Mijdrecht, The Netherlands), and 0.31 mg/kg BW Fentanyl (Janssen-Cilag, Tilburg, The Netherlands). At t = 0 min, blood was taken via tail bleeding and mice were i.v. injected with 100 μl PBS containing 100 μCi Trans^{35}S label (ICM Biomedicals, Irvine, CA, USA) to measure *de novo* total apoB synthesis. After 30 min, the animals received 500 mg of tyloxapol (Triton WR-1339; Sigma-Aldrich) per kilogram body weight as a 10% (w/w) solution in sterile saline, to prevent systemic lipolysis of newly secreted hepatic VLDL-TG. Additional blood samples were taken at t = 15, 30, 60, and 90 min after tyloxapol injection and used for determination of plasma TG concentration. After 90 min, the animals were sacrificed and blood was collected by orbital bleeding for isolation of VLDL by density-gradient ultracentrifugation, as previously described [19-25]. ^{35}S-apoB was measured in the VLDL fraction and VLDL-apoB production rate was calculated as dpm.h^{-1}, as previously reported [19-25].

In vivo clearance of VLDL-like emulsion particles

Mice were fasted overnight with food withdrawn at 06:00 p.m. During the experiment, mice were sedated as described above. At t = 0 min, blood was taken via tail bleeding and mice received a continuous intravenous infusion of glycerol tri[^{3}H]oleate-labeled emulsion particles mixed with albumin-bound [^{14}C]oleic acid (4.4 μCi [^{3}H]TG and 1.2 μCi [^{14}C]FA, both purchased from GE Healthcare Life Sciences, Little Chalfont, UK) at a rate of 100 μl/h for 2.5 h, as previously described [26, 27]. Blood samples were taken using chilled paraoxon-coated capillaries by tail bleeding at 90 and 120 min of infusion to ensure that steady-state conditions had been reached. Subsequently, mice were sacrificed and organs were quickly harvested and snap-frozen in liquid nitrogen. Retention of radioactivity in the saponified tissues was measured per milligram of tissue and corrected for the corresponding plasma-specific activities of [^{3}H]FA and [^{14}C]FA, as described [26, 27].

Hepatic lipid composition

Liver lipids were extracted according to a modified protocol from Bligh and Dyer [28]. Briefly, small liver pieces were homogenized in ice-cold methanol. After centrifugation, lipids were extracted by addition of 1800 µl CH_3OH:$CHCl_3$ (1:3 v/v) to 45 µl homogenate, followed by vigorous vortexing and phase separation by centrifugation (14000 rpm; 15 min at RT). The $CHCl_3$ phase was dried and dissolved in 2% Triton X-100 in water. TG, TC and PL concentrations were measured using commercial kits as described above. Liver lipids were expressed as nmol per mg protein, which was determined using the BCA protein assay kit (Pierce, Rockford, IL, USA).

Western blot analysis

Snap-frozen liver or brown adipose tissue samples (~50 mg) were lysed in ice-cold buffer containing: 50 mM Hepes (pH 7.6), 50 mM NaF, 50 mM KCl, 5 mM NaPPi, 1 mM EDTA, 1 mM EGTA, 1 mM DTT, 5 mM β-glycerophosphate, 1 mM sodium vanadate, 1% NP40 and protease inhibitors cocktail (Complete, Roche, Mijdrecht, The Netherlands). Homogenates were centrifuged (13,200 rpm; 15 min, 4°C) and the protein content of the supernatant was determined using a bicinchoninic acid protein assay kit (BCA Protein Assay Kit, Pierce, Rockford, UK). Proteins (10-50 µg) were separated by 7-10% SDS-PAGE followed by transfer to a polyvinylidene fluoride transfer membrane. Membranes were blocked for 1 h at room temperature in tris-buffered saline tween-20 buffer with 5% non-fat dry milk followed by an overnight incubation with specific antibodies (see Supplemental Table 1). Blots were then incubated with horseradish peroxidase-conjugated secondary antibodies for 1 h at room temperature. Bands were visualized by enhanced chemiluminescence and quantified using Image J (NIH, UK).

AMPK kinase assay

AMPK activity was assayed after immunoprecipitation with specific antibodies directed against α1- or α2-AMPK catalytic subunits (Kinasource, Dundee, Scotland), as previously described [13, 14].

RNA purification and quantitative Reverse Transcription-coupled real-time PCR

RNA was extracted from snap-frozen liver or brown adipose tissue samples (~25 mg) using Tripure RNA Isolation reagent (Roche Molecular Biochemicals, Indianapolis, IN, USA). Total RNA (1-2 µg) was reverse transcribed and quantitative real-time PCR was then performed with SYBR Green Core Kit on a MyIQ thermal cycler (Bio-Rad, Hercules, CA, USA). mRNA expression was normalized to *CypD* mRNA content and expressed as fold change compared to control mice using the ΔΔCT method. All the primers sets used were designed for spanning an exon in order to avoid eventual amplification of gDNA and have an efficiency of ~100±5% (Supplemental Table 2).

Statistical analysis

All data are expressed as mean ± SEM. Statistical analysis was performed using SPSS 17.0 software package for Windows (SPSS, Chicago, IL, USA) with two-tailed unpaired Student's test. Differences between groups were considered statistically significant at $P<0.05$.

RESULTS

Metformin reduces plasma cholesterol and triglycerides levels

To investigate the effect of metformin on lipoprotein metabolism, *E3L.CETP* mice were first fed a cholesterol-rich (0.1%) Western-type diet for 4 weeks and next treated with or without metformin (200 mg/kg BW/day) added to the diet for another 4 weeks. As compared with the control group, metformin did not affect body weight, food intake and plasma glucose, insulin and FA levels throughout the intervention period (Supplemental Figure 1). However, metformin rapidly reduced both plasma TC (-27% and -36% at week 2 and 4, respectively; $P<0.05$) and TG (-26% and -38% at week 2 and 4, respectively; $P<0.05$) in a time-dependent manner (Figure 1A,C). Plasma lipoprotein profile analysis showed that this lipid-lowering effect mostly resulted from a reduction of VLDL particles. In addition, a slight shift in plasma cholesterol profile, from VLDL-C to HDL-C (-37% and +37%, respectively), was evidenced (Figure 1B).

Metformin does not affect hepatic VLDL-TG production

Plasma VLDL-TG levels are determined by the balance between VLDL-TG production by the liver and VLDL-TG clearance by peripheral organs. Therefore, we first assessed the effect of metformin on hepatic VLDL-TG and -apoB production by injecting Trans^{35}S and tyloxapol in 4 h-fasted control and metformin-treated *E3L.CETP* mice. Despite the significantly lower basal plasma TG levels (1.72±0.26 mM versus 2.65±0.36 mM, $P<0.05$; data not shown), metformin did not affect the time-dependent accumulation of plasma TG following tyloxapol injection when compared to control *E3L.CETP* mice (Figure 2A). Therefore, the VLDL-TG production rate, calculated from the slope of the curve, was not significantly different (Figure 2A), although a trend for a slight decrease can eventually be suggested. The rate of VLDL-apoB production (Figure 2B), the ratio of TG-apoB (Figure 2C), as well as the composition of the VLDL particles secreted (Figure 2D), were not significantly altered, indicating that metformin did not affect the hepatic lipidation of VLDL particles. In line with these results, the TG, TC and phospholipid (PL) content in the liver from *E3L.CETP* mice did not significantly differ between the control and metformin groups, although hepatic TC content tended to be decreased in the metformin-treated group (-21%, $P=0.07$; Supplemental Figure 2). Furthermore, in our experimental conditions, metformin treatment did not affect hepatic AMPK activity, as assessed by phosphorylation of Thr172-AMPK and Ser79-Acetyl-CoA Carboxylase (ACC), the main downstream target

of AMPK (Supplemental Figure 2). Finally, the hepatic expression of key genes involved in lipid and lipoprotein metabolism were determined (Table 1). Metformin did not affect FA/TG uptake, synthesis and oxidation genes but significantly down-regulated *Lrp1* and *Scarp1*, both involved in cholesterol uptake. In addition, the expression of *Abca1*, *Lcat* and *Pltp* were also found to be significantly down-regulated by metformin, suggesting that part of the HDL-enhancing effect of the drug could result from subtle changes in hepatic lipoprotein metabolism.

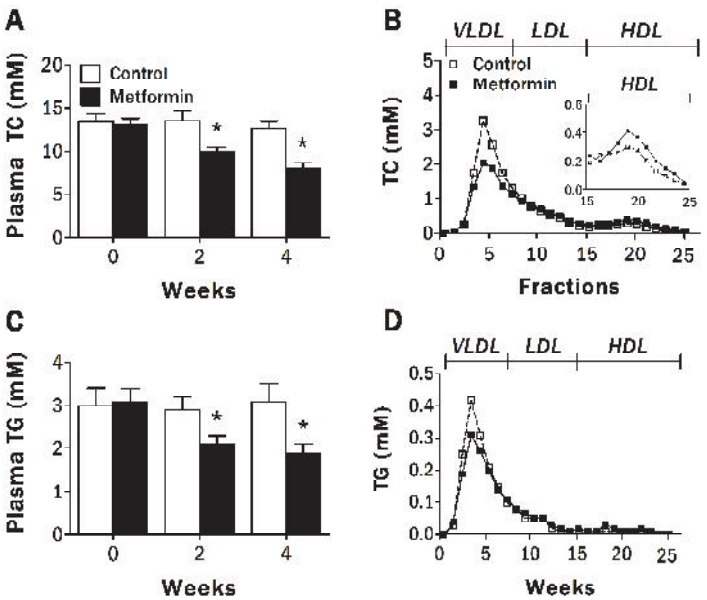

Figure 1. Effect of metformin on plasma cholesterol and triglyceride levels and lipoprotein distribution. Blood samples from 4 h-fasted control (open bars) and metformin-treated (black bars) mice were collected by tail bleeding using chilled paraoxon-coated capillaries at different time-points. Plasma total cholesterol (TC; A) and triglycerides (TG; C) levels were determined. The plasma samples collected after 4 weeks of treatment were pooled group-wise and size-fractionated by fast-protein liquid chromatography. The individual fractions were analysed for cholesterol (B) and TG (D). Data are means ± SEM (n=9/group). * $P<0.05$ vs control.

Metformin promotes VLDL-TG clearance by brown adipose tissue

As clearance of TG from plasma is the other major determinant of TG metabolism, the effect of metformin on whole-body lipid partitioning was next investigated. For this purpose, the tissue-specific retention of FA derived from both [^{3}H]TG-labeled VLDL-like emulsion particles and albumin-bound [^{14}C]FA was determined after continuous tracers infusion for 2.5 h. Strikingly, metformin did not affect the uptake of [^{3}H]TG-derived FA by liver, heart, skeletal muscle and various WAT depots but

markedly increased [^{3}H]TG retention in BAT (+58%, P<0.05; Figure 3A). The uptake of albumin-bound [^{14}C]FA was not different for any of the organs studied (Figure 3B), suggesting that metformin does not affect FA uptake *per se* but rather promotes lipoprotein lipase (LPL)-mediated VLDL-TG hydrolysis in BAT.

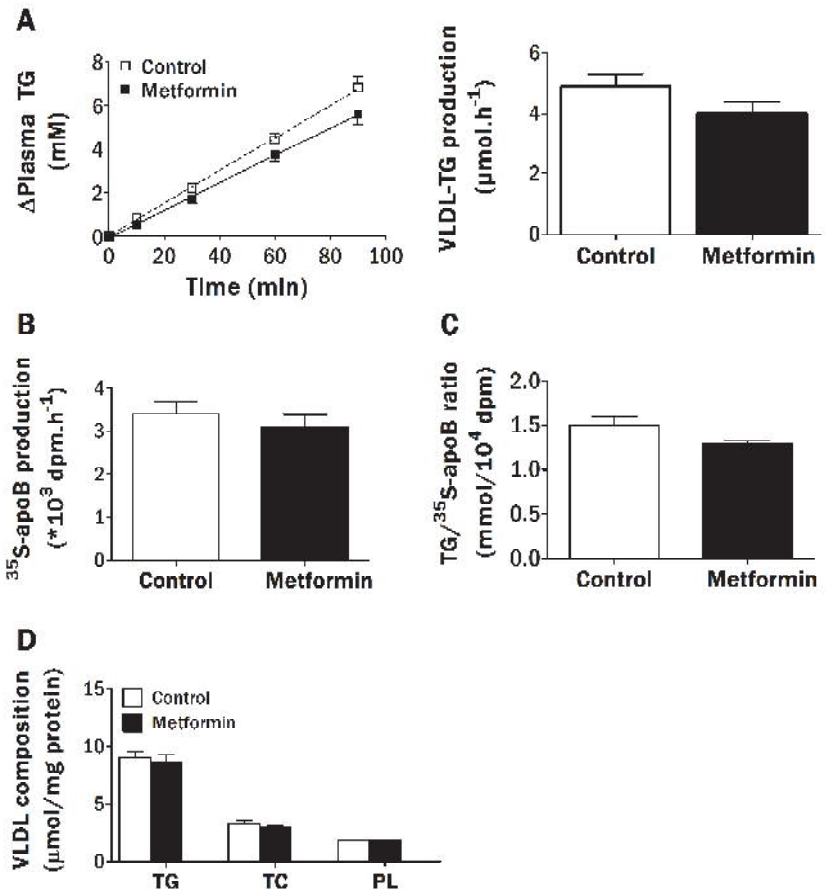

Figure 2. Effect of metformin on hepatic VLDL-TG production. After 4 weeks of treatment, 4 h-fasted control (open squares/bars) and metformin-treated mice (black squares/bars) were injected with Trans^{35}S label (t=-30 min) and tyloxapol (t=0 min), and blood samples were drawn up to 90 min after tyloxapol injection. Plasma TG concentrations were determined and plotted as the increase in plasma TG as compared with baseline (A, left panel). The rate of TG production was calculated from the slopes of the curves from the individual mice (A, right panel). After 120 min, mice were exsanguinated and the total VLDL fraction was isolated by ultracentrifugation. The rate of newly synthesized VLDL-^{35}S-apoB (B), the TG-on-^{35}S-apoB ratio (C), as well as the amount of triglycerides (TG), total cholesterol (TC), and phospholipids (PL) per mg VLDL protein (D) were measured. Data are means ± SEM (n=5-8 per group). ⋆ P<0.05 vs control.

Table 1. Effect of metformin on hepatic expression of genes involved in FA/TG and lipoprotein metabolism. Livers were isolated from 4 h-fasted mice treated with or without metformin for 4 weeks. mRNA expression of the indicated genes were quantified by RT-PCR relative to *CypD* gene and expressed as fold difference compared with the control group. Data are means +/- SEM (n=8). ⋆, P<0.05.

			Fold change	
Function	**Gene**	**Protein**	**Control**	**Metformin**
FA uptake	*Fabp1*	FABP1	1.00 ± 0.16	1.16 ± 0.14
	Cd36	CD36	1.00 ± 0.13	0.89 ± 0.06
	Lpl	LPL	1.00 ± 0.07	0.83 ± 0.10
FA/TG synthesis	*Srebf1*	SREBP-1A	1.00 ± 0.14	0.84 ± 0.16
	Srebf1	SREBP-1C	1.00 ± 0.06	0.94 ± 0.09
	Nr1h3	LXRα	1.00 ± 0.06	0.97 ± 0.04
	Fasn	FAS	1.00 ± 0.16	0.97 ± 0.25
	Scd1	SCD1	1.00 ± 0.22	0.82 ± 0.16
	Dgat1	DGAT1	1.00 ± 0.13	0.89 ± 0.10
FA oxidation	*Pparagc1a*	PGC1α	1.00 ± 0.10	0.72 ± 0.16
	Ppara	PPARα	1.00 ± 0.10	0.93 ± 0.06
	Cpt1a	CPT1α	1.00 ± 0.05	0.94 ± 0.06
	Acaca	ACC1	1.00 ± 0.12	0.83 ± 0.14
	Acacb	ACC2	1.00 ± 0.22	1.07 ± 0.13
	Acox1	ACOX1	1.00 ± 0.06	0.92 ± 0.09
Lipoprotein uptake	*Ldlr*	LDLr	1.00 ± 0.10	0.96 ± 0.12
	Lrp1	LRP1	1.00 ± 0.09	**0.85 ± 0.07⋆**
	Scarb1	SRB1	1.00 ± 0.05	**0.86 ± 0.05⋆**
VLDL synthesis	*Apob*	ApoB	1.00 ± 0.05	0.88 ± 0.07
	Mttp	MTP	1.00 ± 0.10	0.95 ± 0.12
Cholesterol synthesis	*Srbp2*	SRBP2	1.00 ± 0.06	1.07 ± 0.11
	Hmgcr	HMG CoA-R	1.00 ± 0.15	1.13 ± 0.21
	Hmgcs1	HMG CoA-S1	1.00 ± 0.10	1.04 ± 0.18
	Hmgcs2	HMG CoA-S2	1.00 ± 0.06	0.99 ± 0.06
	Sqle	SQLE	1.00 ± 0.20	1.07 ± 0.21
	Idi1	IDI1	1.00 ± 0.10	**1.30 ± 0.10⋆**
	Fdps	FDPS	1.00 ± 0.23	1.21 ± 0.17
	Fdft1	FDFT1	1.00 ± 0.09	0.87 ± 0.14
Cholesterol excretion	*Abcg5*	ABCG5	1.00 ± 0.10	0.82 ± 0.09
	Abcg8	ABCG8	1.00 ± 0.07	0.83 ± 0.12
HDL metabolism	*Apoa1*	ApoA1	1.00 ± 0.10	0.96 ± 0.15
	Lipe	HL	1.00 ± 0.30	0.70 ± 0.16
	Pltp	PLTP	1.00 ± 0.11	**0.78 ± 0.10⋆**
	Abca1	ABCA1	1.00 ± 0.07	**0.78 ± 0.09⋆**
	Lcat	LCAT	1.00 ± 0.04	**0.87 ± 0.06⋆**
	Cetp	CETP	1.00 ± 0.17	0.73 ± 0.20

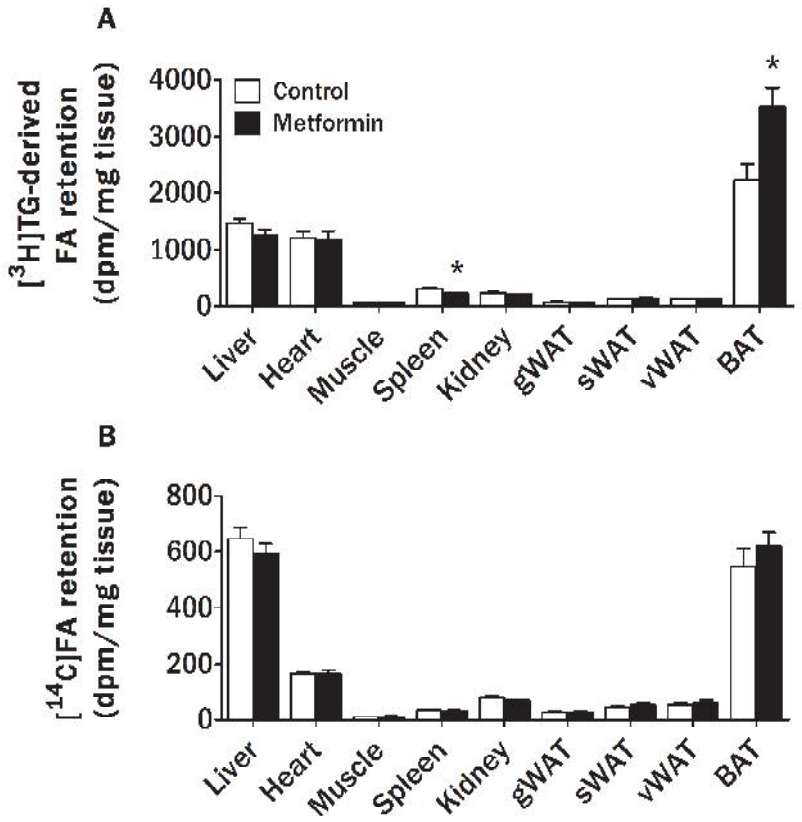

Figure 3. Effect of metformin on peripheral VLDL-TG clearance. 4 h-fasted control (open bars) and metformin-treated (black bars) mice were continuously infused with [^{3}H]TG-labeled VLDL-like emulsion particles mixed with albumin-bound [^{14}C]FA for 2.5 h. Blood samples were taken using chilled paraoxon-coated capillaries by tail bleeding at 90 and 120 min of infusion to ensure that steady-state conditions had been reached. Subsequently, mice were euthanized and organs were quickly harvested and snap-frozen in liquid nitrogen. Plasma levels of TG and FA were determined in plasma and uptake of the radioactively [^{3}H]TG-labeled emulsion particles (A) and albumin-bound [^{14}C]FA (B) was determined in the organs. Data are means ± SEM (n=8 per group). * $P<0.05$ vs control. gWAT, gonadal white adipose tissue; sWAT, subcuataneous white adipose tissue; vWAT, viscerial white adipose tissue; BAT, brown adipose tissue.

Metformin increases AMPK activity and mitochondrial content in brown adipose tissue

To further investigate the molecular mechanism by which metformin increased VLDL-TG clearance by BAT, we determined the mRNA expression of genes involved in FA/lipoprotein uptake, FA metabolism, mitochondrial functions and BAT differentiation, but did not find any significant effect of the drug treatment in our experimental condition (Supplemental Table 3). By contrast, we found that metformin selectively increased the activity of α1- (+19%, $P<0.05$), but not of α2-containing AMPK heterotrimers in BAT (Figure 4A). This was associated with a significant increase in Thr172 phosphorylation (+21%, $P<0.05$) and expression of the AMPKα1

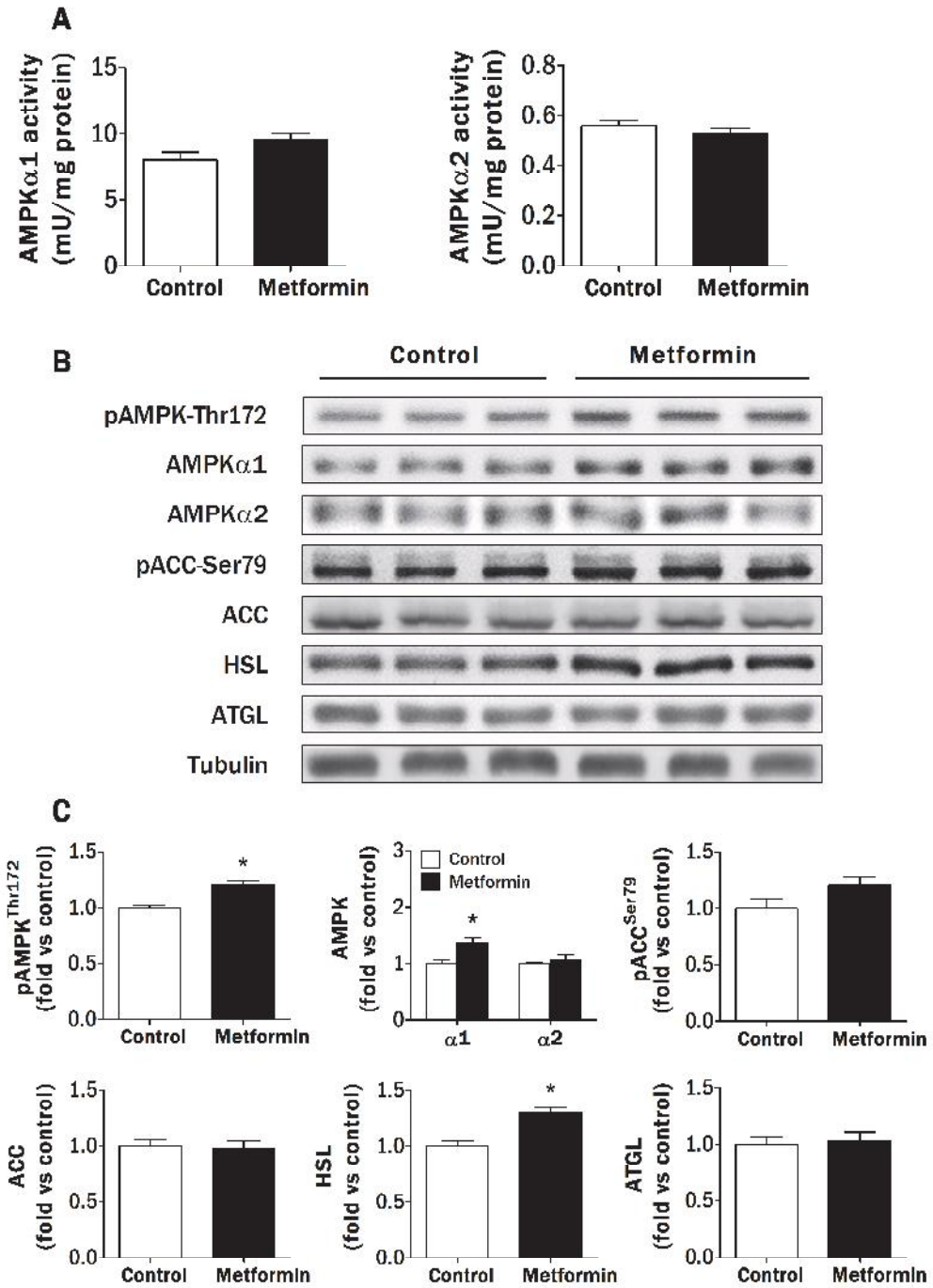

Figure 4. Effect of metformin on AMPK signalling and expression of key lipolytic proteins in brown adipose tissue. Brown adipose tissue from 4 h-fasted mice was collected after 4 weeks of treatment with (black bars) or without metformin (control, open bars) and immediately snap-frozen in liquid nitrogen. The AMPK activity was measured by kinase assay after immunoprecipitation of either AMPKα1 or α2 catalytic subunits with specific antibodies (A). The phosphorylation states of Thr172-AMPK and Ser79-ACC, and the protein expression of AMPKα1, AMPKα2, ACC, HSL and ATGL were assessed in tissue lysate by Western blot (B), followed by densitometric quantification (C). Tubulin expression was used as internal housekeeping protein. Data are means ± SEM (n=8 per group). ⋆ $P<0.05$ vs control.

isoform (+38%, P<0.05), and with a trend for elevated Ser79-phosphorylation of ACC (+21%, P=0.08; Figure 4B-C). We next examined whether some of the key players involved in the regulation of TG lipolysis and FA oxidation in BAT were affected by metformin. Interestingly, the protein expression of the lipolytic enzyme hormone-sensitive lipase (HSL), but not of adipose triglyceride lipase (ATGL), was significantly increased by metformin in BAT (+30%, P<0.05; Figure 4B-C). In addition, we found an increase in protein expression of two of the main regulators of mitochondrial biogenesis, eNOS and PGC-1α (+23% and +127%, respectively; P<0.05), together with a significantly higher mitochondrial content in BAT from metformin-treated *E3L.CETP* mice (+24%, P<0.05) (Figure 5A-B). Of note, the mitochondrial respiratory-chain complex 2-on-1 expression ratio was also increased by metformin in BAT (+17%, P<0.05), whereas the expression of uncoupling protein 1 (UCP1) was unchanged. Taken together, these results show that metformin treatment does not only promote VLDL-TG uptake by BAT but also enhances both intracellular lipolytic and mitochondrial FA β-oxidation capacity in this highly oxidative tissue (Figure 6).

DISCUSSION

Metformin does not only improve glycemic control in type 2 diabetic patients, but also exerts beneficial effects on plasma lipid profiles [29] by a mechanism that remained, so far, poorly understood. In the present study we have therefore investigated the molecular mechanism(s) underlying this lipid-lowering property of metformin using *E3L.CETP* mice, a well-characterized transgenic model displaying a human-like lipoprotein metabolism and human-like responses to lipid-modulating drugs when fed a Western-type diet [19-25]. Our results show that chronic treatment of *E3L.CETP* mice with metformin recapitulates the effects on circulating lipoproteins observed in patients treated with the drug, *i.e* reduction in plasma TG associated with significant reduction in VLDL [30]. We next demonstrated that metformin does not affect hepatic VLDL-TG production, but instead selectively promotes VLDL-TG clearance by BAT, an effect associated with enhanced intracellular lipolysis and FA oxidation machinery in this highly active metabolic tissue. To the best of our knowledge, this study is the first one reporting that BAT is involved in the lipid-lowering effect of metformin, and therefore constitutes an important target tissue for the drug.

Plasma TG levels are determined by the balance between production of chylomicrons and VLDL-TG in intestine and liver, respectively, and their LPL-mediated clearance in peripheral tissues. In our study, all the experiments were performed in fasted mice, thereby excluding any significant contribution of intestine-derived chylomicrons to the change observed in circulating TG concentrations. Furthermore, metformin treatment did not affect the postprandial response to an oral lipid load (Supplemental Figure 3), suggesting that impaired intestinal TG absorption is not involved in the TG-lowering effect of the drug. Besides its central role in glucose homeostasis, the liver

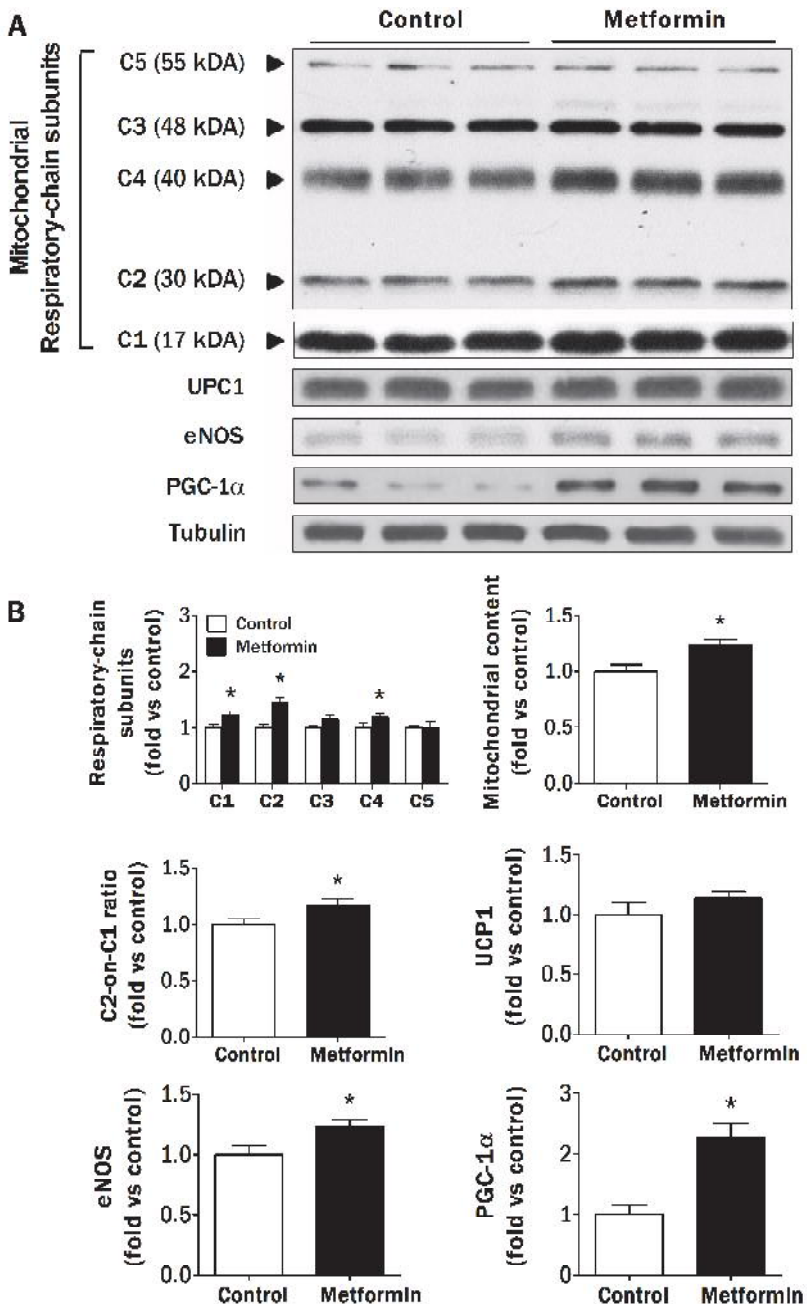

Figure 5. Effect of metformin on key mitochondrial proteins expression in brown adipose tissue. Brown adipose tissue from 4 h-fasted mice was collected after 4 weeks of treatment with (black bars) or without metformin (control, open bars) as described in the legends of Figure 4. The protein expression of various mitochondrial respiratory-chain subunits (CI: NDUFB8; CII: SDHB; CIII: UQCRC2; CIV: MTCO1; CV: ATP5A), and of UCP1, eNOS and PGC-1α were assessed in tissue lysate by Western blot (A), followed by densitometric quantification (B). The mitochondrial tissue content was estimated by the sum of the expression levels of all the mitochondrial respiratory-chain subunits. Tubulin expression was used as internal housekeeping protein. Data are means ± SEM (n=8 per group). ⋆ $P<0.05$ vs control.

plays a key role in lipid metabolism, notably by regulating synthesis and secretion of ApoB-rich VLDL-TG particles [31]. Hepatic VLDL-TG production is mostly driven by intracellular substrate availability resulting from both FA uptake from the circulation and the balance between *de novo* lipogenesis and mitochondrial FA β-oxidation in the liver [32]. In our study, we found that metformin did not significantly affect plasma FA levels, hepatic lipid content, AMPK activity, expression of genes involved in FA/TG uptake, synthesis and oxidation, VLDL-TG and -ApoB secretion rates and composition of the excreted VLDL particles. To our knowledge, these findings are the only data available reporting the *in vivo* effects of chronic metformin treatment on hepatic lipid metabolism and VLDL production in rodents. Although we did not find an apparent contribution of the liver to the TG-reducing effect of metformin, we cannot completely exclude that some of its hepatic effects were lowered or masked due to our experimental conditions, *e.g.* fasting state, and the pharmacokinetic features of the drug. Of note, we found that expression of some genes involved in hepatic HDL uptake (*Lrp1*, *Scarb1*) and remodeling (*Abca1*, *Pltp*) were decreased by metformin, suggesting that part of the mild HDL-raising effect of the drug might be partly due to subtle changes in cholesterol metabolism in the liver. Future studies are required for clarifying the exact underlying molecular mechanism.

Plasma VLDL-TG clearance is driven by LPL-mediated lipolysis in the capillaries of peripheral tissues [33]. The most striking result of our present study was that metformin induced a potent and selective increase in VLDL-TG-derived glycerol tri[^{3}H]oleate retention in BAT without affecting VLDL-TG uptake by heart, muscle and various white adipose tissues. Recently, Bartelt *et al*. were the first to identify BAT as a major organ involved in plasma VLDL-TG clearance in rodents [34]. In this elegant study confirming previous observations [35], they reported that BAT constitutes a quantitatively relevant lipid-clearing organ displaying a very high rates of VLDL-TG uptake [34] by a mechanism that still remains to be fully characterized [36]. In the present study, our observation that metformin promotes VLDL-[^{3}H]TG-derived FA but not albumin-bound [^{14}C]FA retention in BAT suggests that the TG-lowering effect of the drug is mediated by a tissue-specific increase in LPL-mediated VLDL-derived TG hydrolysis. At the molecular level, it remains to be clarified whether increase in endothelial LPL expression and/or subtle changes in apolipoproteins and angiopoietin-like proteins regulating local LPL activity [37] are involved in the BAT-specific VLDL-derived TG hydrolysis induced by metformin.

Owing to its high mitochondrial and oxidative enzyme content, BAT has a marked ability to oxidize both glucose and FA, the latter being either derived from LPL-mediated hydrolysis of VLDL-TG or intracellular TG that are stored in lipid droplets. Once released, FA are rapidly re-esterified in TG or directed to mitochondria for oxidation or activation of UCP1, leading to dissipation of the proton gradient across the inner mitochondrial membrane and heat production [38]. At the molecular level, we found that metformin significantly increased AMPKα1 activity and Ser79-ACC phosphorylation, an effect that is expected to promote mitochondrial FA transport

and oxidation by relieving the inhibition of CPT1α by malonyl-CoA [9]. AMPK activation is known to trigger mitochondrial biogenesis, at least in skeletal muscle [39] and liver [40]. Interestingly, the expression of key proteins of the mitochondrial respiratory-chain complexes, but not UCP1, was increased by metformin in BAT, indicating enhanced mitochondrial content in this tissue. Mechanistically, the expression of PGC-1α and eNOS, which are both recognized as important regulators of mitochondrial biogenesis [41, 42] were found to be higher in BAT of metformin-treated mice, suggesting activation of the AMPK-PGC1α-eNOS pathway by metformin in this tissue. Finally, we found that metformin affected the qualitative composition of the mitochondrial respiratory chain in BAT, leading to an increase in complex 2 relative to complex 1. This effect might also contribute to enhanced FA oxidation by promoting electron supply to the respiratory chain complex 2. Interestingly, modulating the ratio of FADH2-to-NADH oxidation will also affect the stoichiometry of oxidative phosphorylation and promote metabolic uncoupling, with the yield of ATP synthesis being lowered by approximately 40% when FADH2 is oxidized as compared to NADH [43]. Taken together, we propose that secondary to its tissue-specific increase in VLDL-TG uptake, metformin promotes FA oxidation in BAT by enhancing both intracellular lipolytic capacity and mitochondrial oxidative machinery.

The recent discovery of active BAT in adult humans [44-47] has caused a revival interest in this potential new therapeutic target for the treatment of obesity and metabolic disorders [48]. Interestingly, in contrast to other glucose-lowering agents such as sulphonylureas, glitazones or insulin, metformin treatment often results in significant weight loss in obese diabetic patients. It is therefore tempting to speculate that part of the weight-lowering property of the drug might be secondary to enhanced lipid oxidation and energy dissipation in BAT. Further studies allowing imaging of lipid metabolism in BAT from metformin-treated patients, for instance using ^{18}F-labeled FA incorporated into VLDL-TG coupled to position emission tomography scanning [49], would be crucial to specifically address this point.

In summary, we demonstrate in the present study that metformin exerts a beneficial effect on circulating lipids by lowering plasma TG, through a selective BAT-mediated increase in VLDL-TG uptake/lipolysis (Figure 6). The present study is the first identifying BAT as a new important mechanistic player in the lipid-lowering action of metformin, suggesting that targeting this tissue, on top of being interesting for body weight management, might also be of therapeutic importance in the treatment of dyslipidemia.

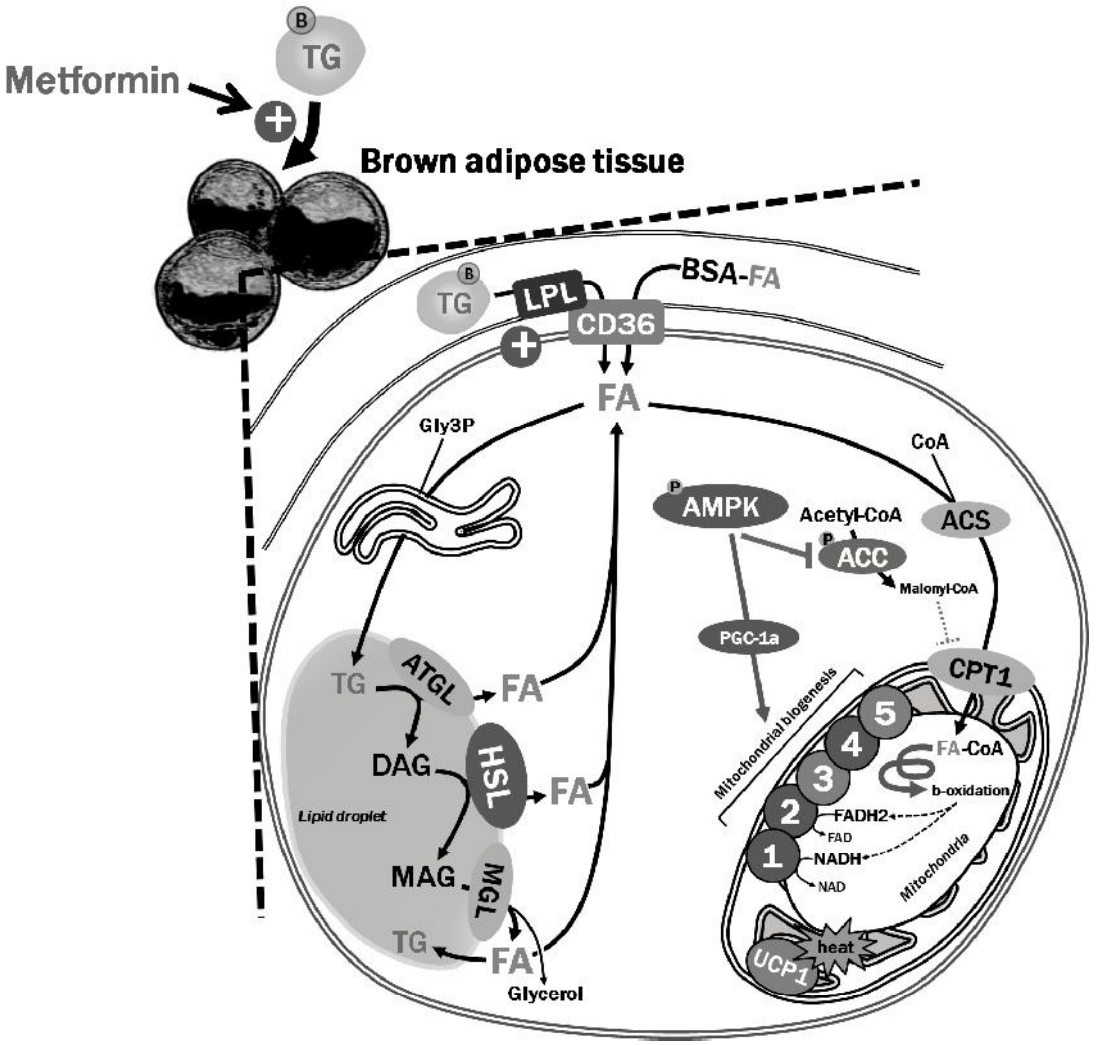

Figure 6. Proposed mechanism for the brown adipose tissue-mediated TG-lowering effect of metformin. Metformin exerts a beneficial effect on circulating lipids by lowering plasma TG, through a selective increase in TG-derived FA uptake by BAT. In addition, metformin also improves intracellular lipolytic capacity by increasing HSL expression, thereby enhancing FA release from TG stored in lipid droplets. We propose that metformin next promotes FA oxidation in BAT by multiple (path)ways. First, metformin activates AMPKα1, leading to the subsequent phosphorylation and inactivation of its downstream target ACC. This relieves the inhibition exerted by malonyl-CoA on CPT1, ultimately promoting mitochondrial FA transport and oxidation. Second, metformin increases the tissue mitochondrial content, an effect that might be due to AMPK-mediated stimulation of mitochondrial biogenesis, as reflected by higher expression of eNOS and PGC-1α. Finally, by changing the qualitative composition of the mitochondrial respiratory-chain, metformin can enhance respiratory-chain complex 2-mediated FA oxidation and metabolic uncoupling of oxidative phosphorylation.

ACKNOWLEDGEMENTS

The authors are grateful to Elsbet Pieterman, Chris van der Bent and Amanda Pronk for their valuable technical assistance. This work was supported by a SFD-Roche Diagnostics grant from the Société Francophone du Diabète (SFD) to BG, and by a research grant from the Netherlands Diabetes Foundation (DFN2007.00.010 to PCNR). PCNR is an Established Investigator of the Netherlands Heart Foundation (grant 2009T038).

REFERENCES

1. Goodarzi MO, Bryer-Ash M: Metformin revisited: re-evaluation of its properties and role in the pharmacopoeia of modern antidiabetic agents. Diabetes Obes Metab 2005;7:654-665
2. Nathan DM, Buse JB, Davidson MB, Ferrannini E, Holman RR, Sherwin R, Zinman B: Medical management of hyperglycaemia in type 2 diabetes mellitus: a consensus algorithm for the initiation and adjustment of therapy: a consensus statement from the American Diabetes Association and the European Association for the Study of Diabetes. Diabetologia 2009;52:17-30
3. Natali A, Ferrannini E: Effects of metformin and thiazolidinediones on suppression of hepatic glucose production and stimulation of glucose uptake in type 2 diabetes: a systematic review. Diabetologia 2006;49:434-441
4. Salpeter SR, Buckley NS, Kahn JA, Salpeter EE: Meta-analysis: metformin treatment in persons at risk for diabetes mellitus. Am J Med 2008;121:149-157 e142
5. UKPDS: Effect of intensive blood-glucose control with metformin on complications in overweight patients with type 2 diabetes (UKPDS 34). UK Prospective Diabetes Study (UKPDS) Group. Lancet 1998a;352:854-865
6. Viollet B, Guigas B, Sanz Garcia N, Leclerc J, Foretz M, Andreelli F: Cellular and molecular mechanisms of metformin: an overview. Clin Sci (Lond) 2012;122:253-270
7. Zhou G, Myers R, Li Y, Chen Y, Shen X, Fenyk-Melody J, Wu M, Ventre J, Doebber T, Fujii N, Musi N, Hirshman MF, Goodyear LJ, Moller DE: Role of AMP-activated protein kinase in mechanism of metformin action. J Clin Invest 2001;108:1167-1174
8. Carling D, Thornton C, Woods A, Sanders MJ: AMP-activated protein kinase: new regulation, new roles? Biochem J 2012;445:11-27
9. Hardie DG, Ross FA, Hawley SA: AMPK: a nutrient and energy sensor that maintains energy homeostasis. Nat Rev Mol Cell Biol 2012;13:251-262
10. El-Mir MY, Nogueira V, Fontaine E, Averet N, Rigoulet M, Leverve X: Dimethylbiguanide inhibits cell respiration via an indirect effect targeted on the respiratory chain complex I. J Biol Chem 2000;275:223-228
11. Owen MR, Doran E, Halestrap AP: Evidence that metformin exerts its anti-diabetic effects through inhibition of complex 1 of the mitochondrial respiratory chain. Biochem J 2000;348 Pt 3:607-614
12. Hawley SA, Ross FA, Chevtzoff C, Green KA, Evans A, Fogarty S, Towler MC, Brown LJ, Ogunbayo OA, Evans AM, Hardie DG: Use of cells expressing gamma subunit variants to identify diverse mechanisms of AMPK activation. Cell Metab 2010;11:554-565
13. Stephenne X, Foretz M, Taleux N, van der Zon GC, Sokal E, Hue L, Viollet B, Guigas B: Metformin activates AMP-activated protein kinase in primary human hepatocytes by decreasing cellular energy status. Diabetologia 2011;54:3101-3110
14. Guigas B, Bertrand L, Taleux N, Foretz M, Wiernsperger N, Vertommen D, Andreelli F, Viollet B, Hue L: 5-Aminoimidazole-4-carboxamide-1-beta-D-ribofuranoside and metformin inhibit hepatic glucose phosphorylation by an AMP-activated protein kinase-independent effect on glucokinase translocation. Diabetes 2006;55:865-874
15. Foretz M, Hebrard S, Leclerc J, Zarrinpashneh E, Soty M, Mithieux G, Sakamoto K, Andreelli F, Viollet B: Metformin inhibits hepatic gluconeogenesis in mice independently of the LKB1/AMPK pathway via a decrease in hepatic energy state. J Clin Invest 2010;120:2355-2369
16. Shaw RJ, Lamia KA, Vasquez D, Koo SH, Bardeesy N, Depinho RA, Montminy M, Cantley LC: The kinase LKB1 mediates glucose homeostasis in liver and therapeutic effects of metformin. Science 2005;310:1642-1646
17. Kalender A, Selvaraj A, Kim SY, Gulati P, Brule S, Viollet B, Kemp BE, Bardeesy N, Dennis P, Schlager JJ, Marette A, Kozma SC, Thomas G: Metformin, independent of AMPK, inhibits mTORC1 in a rag GTPase-dependent manner. Cell Metab 2010;11:390-401
18. Miller RA, Chu Q, Xie J, Foretz M, Viollet B, Birnbaum MJ: Biguanides suppress hepatic glucagon signalling by decreasing production of cyclic AMP. Nature 2013;

19. Westerterp M, van der Hoogt CC, de Haan W, Offerman EH, Dallinga-Thie GM, Jukema JW, Havekes LM, Rensen PC: Cholesteryl ester transfer protein decreases high-density lipoprotein and severely aggravates atherosclerosis in APOE*3-Leiden mice. Arterioscler Thromb Vasc Biol 2006;26:2552-2559
20. Bijland S, Pieterman EJ, Maas AC, van der Hoorn JW, van Erk MJ, van Klinken JB, Havekes LM, van Dijk KW, Princen HM, Rensen PC: Fenofibrate increases very low density lipoprotein triglyceride production despite reducing plasma triglyceride levels in APOE*3-Leiden.CETP mice. J Biol Chem 2010;285:25168-25175
21. Bijland S, Rensen PC, Pieterman EJ, Maas AC, van der Hoorn JW, van Erk MJ, Havekes LM, Willems van Dijk K, Chang SC, Ehresman DJ, Butenhoff JL, Princen HM: Perfluoroalkyl sulfonates cause alkyl chain length-dependent hepatic steatosis and hypolipidemia mainly by impairing lipoprotein production in APOE*3-Leiden CETP mice. Toxicol Sci 2011;123:290-303
22. Bijland S, van den Berg SA, Voshol PJ, van den Hoek AM, Princen HM, Havekes LM, Rensen PC, Willems van Dijk K: CETP does not affect triglyceride production or clearance in APOE*3-Leiden mice. J Lipid Res 2010;51:97-102
23. de Haan W, de Vries-van der Weij J, Mol IM, Hoekstra M, Romijn JA, Jukema JW, Havekes LM, Princen HM, Rensen PC: PXR agonism decreases plasma HDL levels in ApoE3-Leiden.CETP mice. Biochim Biophys Acta 2009;1791:191-197
24. de Haan W, van der Hoogt CC, Westerterp M, Hoekstra M, Dallinga-Thie GM, Princen HM, Romijn JA, Jukema JW, Havekes LM, Rensen PC: Atorvastatin increases HDL cholesterol by reducing CETP expression in cholesterol-fed APOE*3-Leiden.CETP mice. Atherosclerosis 2008;197:57-63
25. van der Hoorn JW, de Haan W, Berbee JF, Havekes LM, Jukema JW, Rensen PC, Princen HM: Niacin increases HDL by reducing hepatic expression and plasma levels of cholesteryl ester transfer protein in APOE*3Leiden.CETP mice. Arterioscler Thromb Vasc Biol 2008;28:2016-2022
26. Teusink B, Voshol PJ, Dahlmans VE, Rensen PC, Pijl H, Romijn JA, Havekes LM: Contribution of fatty acids released from lipolysis of plasma triglycerides to total plasma fatty acid flux and tissue-specific fatty acid uptake. Diabetes 2003;52:614-620
27. Coomans CP, Geerling JJ, Guigas B, van den Hoek AM, Parlevliet ET, Ouwens DM, Pijl H, Voshol PJ, Rensen PC, Havekes LM, Romijn JA: Circulating insulin stimulates fatty acid retention in white adipose tissue via K_{ATP} channel activation in the central nervous system only in insulin-sensitive mice. J Lipid Res 2011;52:1712-1722
28. Bligh EG, Dyer WJ: A rapid method of total lipid extraction and purification. Can J Biochem Physiol 1959;37:911-917
29. Buse JB, Tan MH, Prince MJ, Erickson PP: The effects of oral anti-hyperglycaemic medications on serum lipid profiles in patients with type 2 diabetes. Diabetes, obesity & metabolism 2004;6:133-156
30. Jonker JT, Wang Y, de Haan W, Diamant M, Rijzewijk LJ, van der Meer RW, Lamb HJ, Tamsma JT, de Roos A, Romijn JA, Rensen PC, Smit JW: Pioglitazone decreases plasma cholesteryl ester transfer protein mass, associated with a decrease in hepatic triglyceride content, in patients with type 2 diabetes. Diabetes Care 2010;33:1625-1628
31. Xiao C, Hsieh J, Adeli K, Lewis GF: Gut-liver interaction in triglyceride-rich lipoprotein metabolism. Am J Physiol Endocrinol Metab 2011;301:E429-446
32. Nielsen S, Karpe F: Determinants of VLDL-triglycerides production. Curr Opin Lipidol 2012;23:321-326
33. Dallinga-Thie GM, Franssen R, Mooij HL, Visser ME, Hassing HC, Peelman F, Kastelein JJ, Peterfy M, Nieuwdorp M: The metabolism of triglyceride-rich lipoproteins revisited: new players, new insight. Atherosclerosis 2010;211:1-8
34. Bartelt A, Bruns OT, Reimer R, Hohenberg H, Ittrich H, Peldschus K, Kaul MG, Tromsdorf UI, Weller H, Waurisch C, Eychmuller A, Gordts PL, Rinninger F, Bruegelmann K, Freund B, Nielsen P, Merkel M, Heeren J: Brown adipose tissue activity controls triglyceride clearance. Nat Med 2011;17:200-205

35. Hagberg CE, Falkevall A, Wang X, Larsson E, Huusko J, Nilsson I, van Meeteren LA, Samen E, Lu L, Vanwildemeersch M, Klar J, Genove G, Pietras K, Stone-Elander S, Claesson-Welsh L, Yla-Herttuala S, Lindahl P, Eriksson U: Vascular endothelial growth factor B controls endothelial fatty acid uptake. Nature 2010;464:917-921
36. Bartelt A, Merkel M, Heeren J: A new, powerful player in lipoprotein metabolism: brown adipose tissue. J Mol Med (Berl) 2012;90:887-893
37. Davies BS, Beigneux AP, Fong LG, Young SG: New wrinkles in lipoprotein lipase biology. Curr Opin Lipidol 2012;23:35-42
38. Festuccia WT, Blanchard PG, Deshaies Y: Control of Brown Adipose Tissue Glucose and Lipid Metabolism by PPARgamma. Front Endocrinol (Lausanne) 2011;2:84
39. Zong H, Ren JM, Young LH, Pypaert M, Mu J, Birnbaum MJ, Shulman GI: AMP kinase is required for mitochondrial biogenesis in skeletal muscle in response to chronic energy deprivation. Proc Natl Acad Sci U S A 2002;99:15983-15987
40. Guigas B, Taleux N, Foretz M, Detaille D, Andreelli F, Viollet B, Hue L: AMP-activated protein kinase-independent inhibition of hepatic mitochondrial oxidative phosphorylation by AICA riboside. Biochem J 2007;404:499-507
41. Lira VA, Brown DL, Lira AK, Kavazis AN, Soltow QA, Zeanah EH, Criswell DS: Nitric oxide and AMPK cooperatively regulate PGC-1 in skeletal muscle cells. J Physiol 2010;588:3551-3566
42. Seale P, Kajimura S, Spiegelman BM: Transcriptional control of brown adipocyte development and physiological function--of mice and men. Genes Dev 2009;23:788-797
43. Leverve XM, Taleux N, Favier R, Batandier C, Detaille D, Devin A, Fontaine E, Rigoulet M: Cellular energy metabolism and integrated oxidative phosphorylation. In Molecular system bioenergetics: Energy for life Saks V, Ed. Weinheim, WILEY-VCH Verlag GmbH & Co, 2007, p. 11-27
44. Cypess AM, Lehman S, Williams G, Tal I, Rodman D, Goldfine AB, Kuo FC, Palmer EL, Tseng YH, Doria A, Kolodny GM, Kahn CR: Identification and importance of brown adipose tissue in adult humans. N Engl J Med 2009;360:1509-1517
45. Nedergaard J, Bengtsson T, Cannon B: Unexpected evidence for active brown adipose tissue in adult humans. Am J Physiol Endocrinol Metab 2007;293:E444-452
46. van Marken Lichtenbelt WD, Vanhommerig JW, Smulders NM, Drossaerts JM, Kemerink GJ, Bouvy ND, Schrauwen P, Teule GJ: Cold-activated brown adipose tissue in healthy men. N Engl J Med 2009;360:1500-1508
47. Virtanen KA, Lidell ME, Orava J, Heglind M, Westergren R, Niemi T, Taittonen M, Laine J, Savisto NJ, Enerback S, Nuutila P: Functional brown adipose tissue in healthy adults. N Engl J Med 2009;360:1518-1525
48. Ravussin E, Galgani JE: The implication of brown adipose tissue for humans. Annu Rev Nutr 2011;31:33-47
49. Labbe SM, Grenier-Larouche T, Croteau E, Normand-Lauziere F, Frisch F, Ouellet R, Guerin B, Turcotte EE, Carpentier AC: Organ-specific dietary fatty acid uptake in humans using positron emission tomography coupled to computed tomography. Am J Physiol Endocrinol Metab 2011;300:E445-453

SUPPLEMENTAL DATA

Supplemental Table 1. Antibodies used for Western blots

Primary antibody	Residue	Supplier	Reference	Dilution
ACC	-	Cell Signaling	#3662	1:2000
ACC	Ser79	Cell Signaling	#3661	1:2000
AMPKα	Thr172	Cell Signaling	#2535	1:1000
AMPKα	-	Cell Signaling	#2532	1:1000
AMPKα1	-	Kinasource	AB-140	1:2500
AMPKα2	-	Kinasource	AB-141	1:2500
ATGL	-	Cell Signaling	#2439	1:1250
eNOS (NOS3)	-	Santa Cruz	sc-654	1:1000
HSL	-	Cell Signaling	#4107	1:2000
MitoProfile	-	AbCam	ab110413	1:1000
UCP1	-	Sigma	U6382	1:2500
Tubulin	-	Cell Signaling	#2148	1:2000

Supplemental Table 2. qPCR primers

Gene	Accession nr.	Forward primer	Reverse primer
Abca1	NM_013454.3	CCCAGAGCAAAAAGCGACTC	GGTCATCATCACTTTGGTCCTTG
Abcg5	NM_031884	TGTCCTACAGCGTCAGCAACC	GGCCACTCTCGATGTACAAGG
Abcg8	NM_026180	TCCTGTGAGCTGGGCATCCGA	CCCGCAGCCTGAGCTCCCTAT
Acaca	NM_133360.2	CAGCTGGTGCAGAGGTACCG	TCTACTCGCAGGTACTGCCG
Acacb	NM_133904.2	GCGCCTACTATGAGGCCCAGCA	ACAAACTCGGCTGGGGACGC
Acly	NM_134037.2	TGTGGACGGCTTCATCGGCG	ATGTCATCCCAGGGGTGACG
Acox1	NM_015729	GGGACCCACAAGCCTCTGCCA	GTGCCGTCAGGCTTCACCTGG
Apoa1	NM_009692	TGCGGTCAAAGACAGCGGCA	AGATTCAGGTTCAGCTGTTGGCCC
Apob	NM_009693	CAGCTGCAAGTGTCCTCGTC	GACACAGAGGGCTTTGCCAC
Atp5a1	NM_007505.2	CCAAGCAGGCTGTCGCTTACCG	TCTCCAGCAGGCGGGAGTGT
Cd36	NM_001159558	GCAAAGAACAGCAGCAAAATC	CAGTGAAGGCTCAAAGATGG
Cox7a1	NM_009944.3	AAAACCGTGTGGCAGAGAAG	CCAGCCCAAGCAGTATAAGC
Cpt1a	NM_013495	AGGAGACAAGAACCCCAACA	AAGGAATGCAGGTCCACATC
Creb1	NM_133828	AGCTGCCACTCAGCCGGGTA	TCGCCTGAGGCAGCTTGAACA
Dgat1	NM_010046.2	CTAGTGAGCGTTCCCCTGCG	GGGCATCGTAGTTGAGCACG
Dio2	NM_010050	CGCTCCAAGTCCACTCGCGG	CGGCCCCATCAGCGGTCTTC
Fabp1	NM_017399.4	GCCACCATGAACTTCTCCGGCA	GGTCCTCGGGCAGACCTATTGC
Fasn	NM_007988	CACAGGCATCAATGTCAACC	TTTGGGAAGTCCTCAGCAAC
Fdft1	NM_010191.2	CCAACTCAATGGGTCTGTTCCT	TGGCTTAGCAAAGTCTTCCAACT
Fdps	NM_134469.4	ATGGAGATGGGCGAGTTCTTC	CCGACCTTTCCCGTCACA
Gpam	NM_008149.3	TCATACCCGTGGGCATCTCG	AATCCACTCGGACGTAGCCG
Gpihbp1	NM_026730	AGTGGACAGCCAGGGAGTGGC	GCTCTCCCCGCTGTGAAGCAC
Hmgcr	NM_008255	CTTGTGGAATGCCTTGTGATTG	AGCCGAAGCAGCACATGAT
Hmgcs1	NM_145942.4	GGACTGGAAGCCTTTGGGGACG	TGCCAGGACAGAAGCCAGGGA
Hmgcs2	NM_008256.4	CATCGCAGGAAGTATGCCCG	GCTGTTTGGGTAGCAGCTCG
Idi1	NM_145360.2	TGGGAATACCCTTGGAAGAGGTTGA	CCCCAGATACCATCAGATTGGGCCT
Lcat	NM_008490.2	GGCAAGACCGAATCTGTTGAG	ACCAGATTCTGCACCAGTGTGT
Ldlr	NM_010700	GCATCAGCTTGGACAAGGTGT	GGGAACAGCCACCATTGTTG
Lipe	NM_010719	AGCCTCATGGACCCTCTTCT	GCCTAGTGCCTTCTGGTCTG
Lpl	NM_008509	CAGGGGGTCACCTGGTCGAAGT	AGCTGGTCCACGTCTCCGAGT
Lrp1	NM_008512	GGAACTCCAGTCGCTGCAAC	TAGCACAGGGATGTCCGCTC
Mttp	NM_008642	GCCTGTGGCTTTGCCACCCA	TCCACCACTGCCTTGAGCTTGC
Ndufb8	NM_026061.2	GAGGCACGGAGAGCCTTCCA	GGGAGCATCGGGTAGTCGCC
Nr1h3	NM_013839.4	CTGCACGCCTACGTCTCCAT	AAGTACGGAGGCTCACCAGCT
Pltp	NM_011125.2	GGCCGTCTCAGTGCTAAGTT	CGAAGTTGATACCCTCAGGAA

(continued on next page)

Supplemental Table 2. qPCR primers (continued)

Gene	Accession nr.	Forward primer	Reverse primer
Ppara	NM_011144	CAACCCGCCTTTTGTCATAC	CCTCTGCCTCTTTGTCTTCG
Pparg	NM_011146	CCTGCGGAAGCCCTTTGGTGA	AGCCTGGGCGGTCTCCACTG
Ppargc1a	NM_008904.2	TGCTAGCGGTTCTCACAGAG	AGTGCTAAGACCGCTGCATT
Ppargc1b	NM_133249	CTTGCTTTTCCCAGATGAGG	CCCTGTCCGTGAGGAACG
Ppargc1b	NM_133249	CTTGCTTTTCCCAGATGAGG	CCCTGTCCGTGAGGAACG
Prkaa1	NM_001013367	TGGTGGGAAAAATCCGCCGGG	CGGCTTTCCTTTTCGTCCAACCTTC
Prkaa2	NM_178143	ACCGAGCTATGAAGCAGCTGGGTT	CCTCTGCTCCACCACCTCATCATC
Scarb1	NM_016741	TCGCTTCACGGCCCCCGATA	ACAGAGGCGCACCAAACCTGC
Scd1	NM_009127.4	GCTCTACACCTGCCTCTTCGGGAT	TCCAGAGGCGATGAGCCCCG
Sdha	NM_023281.1	GGGACAGGTGCTGAAGCATGTGAAT	GCAATGCTCAGGGCACAGGCT
Sdhb	NM_023374.3	CGACGGTCGGGGTCTCCTTGA	CCTGAAACTGCAGGCCGACTC
Sqle	NM_009270.3	TCGTTCGTGACGGACCCGGA	ACTGTATCTCCAAGGCCCAGCTCC
Srebf1	NM_011480	GGCCGAGATGTGCGAACT	TTGTTGATGAGCTGGAGCATGT
Srebf1	NM_011480	CTGGCTGAGGCGGGATGA	TACGGGCCACAAGAAGTAGA
Tfam	NM_009360	CTTCCTGGGTTCACCCGCAC	ATGGGCACTATGGCTCCGTC
Ucp1	NM_009463	TCAGGATTGGCCTCTACGAC	TGCATTCTGACCTTCACGAC
Vldlr	NM_013703	TCTTGAGCAGTGTGGCCGTC	TTGCAGTCAGGGTCTCCGTC

Supplemental Table 3. Metformin does not affect expression of genes involved in tissue differentiation, lipoprotein/FA uptake, TG synthesis, FA oxidation and mitochondrial functions in brown adipose tissue. Brown adipose tissues were isolated from 4 h-fasted mice treated with or without metformin for 4 weeks. mRNA expression of the indicated genes were quantified by RT-PCR relative to *CypD* gene and expressed as fold difference compared with the control group. Data are means +/- SEM (n=8).

			Fold change	
Function	**Gene**	**Protein**	**Control**	**Metformin**
BAT differentiation	*Prdm16*	PRDM16	1.00 ± 0.27	1.14 ± 0.35
	Cidea	CIDEA	1.00 ± 0.20	1.09 ± 0.20
	Dio2	DIO2	1.00 ± 0.16	1.00 ± 0.20
	Essra	ESSRα	1.00 ± 0.36	1.03 ± 0.43
Lipoprotein/FA uptake	*CD36*	CD36	1.00 ± 0.11	0.90 ± 0.12
	Ldlr	LDLr	1.00 ± 0.20	1.19 ± 0.29
	Lrp1	LRP1	1.00 ± 0.09	1.34 ± 0.34
	Vldlr	VLDLr	1.00 ± 0.12	0.96 ± 0.11
	Gpihbp1	GPIHBP1	1.00 ± 0.05	1.17 ± 0.13
	Lpl	LPL	1.00 ± 0.16	0.96 ± 0.22
FA/TG synthesis	*Scd1*	SCD1	1.00 ± 0.17	0.94 ± 0.26
	Fasn	FAS	1.00 ± 0.14	1.25 ± 0.22
	Acly	ACLY	1.00 ± 0.23	0.94 ± 0.18
	Dgat1	DGAT1	1.00 ± 0.16	1.10 ± 0.13
	Pck1	PEPCK	1.00 ± 0.18	1.18 ± 0.26
	Gpam	GPAT	1.00 ± 0.23	1.03 ± 0.31
FA oxidation	*Ppara*	PPARα	1.00 ± 0.23	1.15 ± 0.25
	Pparg	PPARγ	1.00 ± 0.06	1.06 ± 0.08
	Cpt1a	CPT1α	1.00 ± 0.20	0.98 ± 0.31
	Prkaa1	AMPKα1	1.00 ± 0.12	1.11 ± 0.14
	Prkaa2	AMPKα2	1.00 ± 0.20	1.09 ± 0.14
	Acaca	ACC1	1.00 ± 0.19	1.12 ± 0.19
	Acacb	ACC2	1.00 ± 0.19	1.25 ± 0.26
Mitochondria	*Pparagc1a*	PGC1α	1.00 ± 0.25	1.01 ± 0.21
	Tfam	Tfam	1.00 ± 0.13	0.96 ± 0.17
	Ucp1	UCP1	1.00 ± 0.12	1.13 ± 0.05
	Cox7a1	COX7	1.00 ± 0.11	1.05 ± 0.07
	Atp5a1	ATP5A1	1.00 ± 0.09	0.99 ± 0.09
	Ndufb8	NDUFB8	1.00 ± 0.13	0.98 ± 0.13
	Sdha	SDHA	1.00 ± 0.10	1.06 ± 0.21
	Sdhb	SDHB	1.00 ± 0.12	0.90 ± 0.10
	Uqcrc2	UQCRC2	1.00 ± 0.08	1.04 ± 0.07

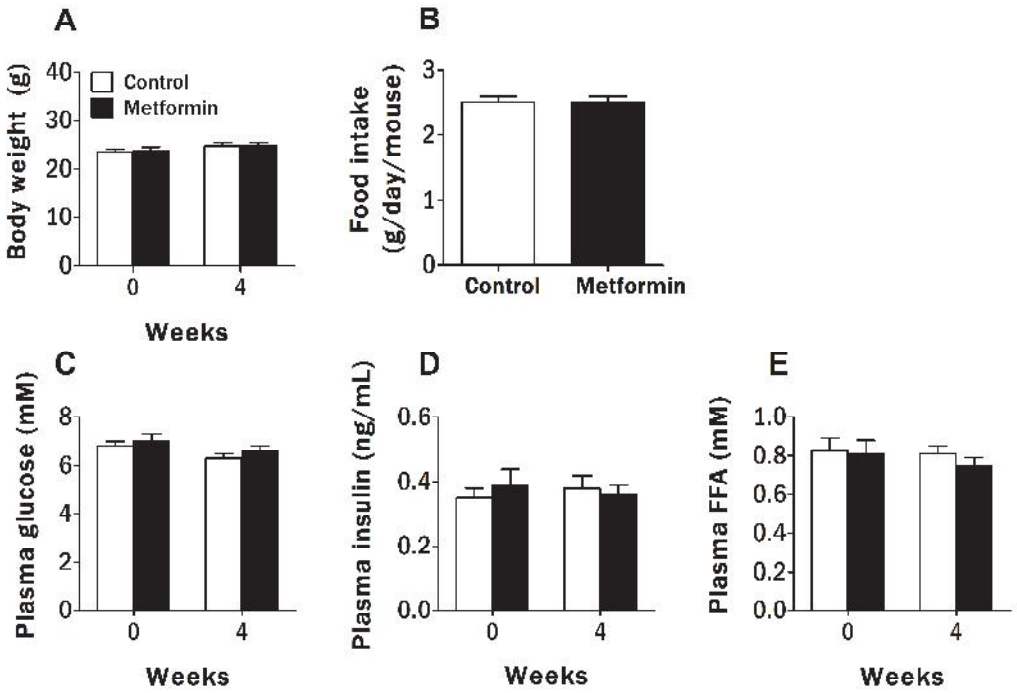

Supplemental Figure 1. Effect of metformin on body weight, food intake and various plasma parameters. Body weight (A) and mean food intake (B) were measured throughout the study in control (open bars) and metformin-treated (black bars) mice. Blood samples were collected as described in Figure 1 and plasma glucose (C), insulin (D) and free fatty acids (FFA; E) levels were determined. Values are means ± SEM (n=9/group).

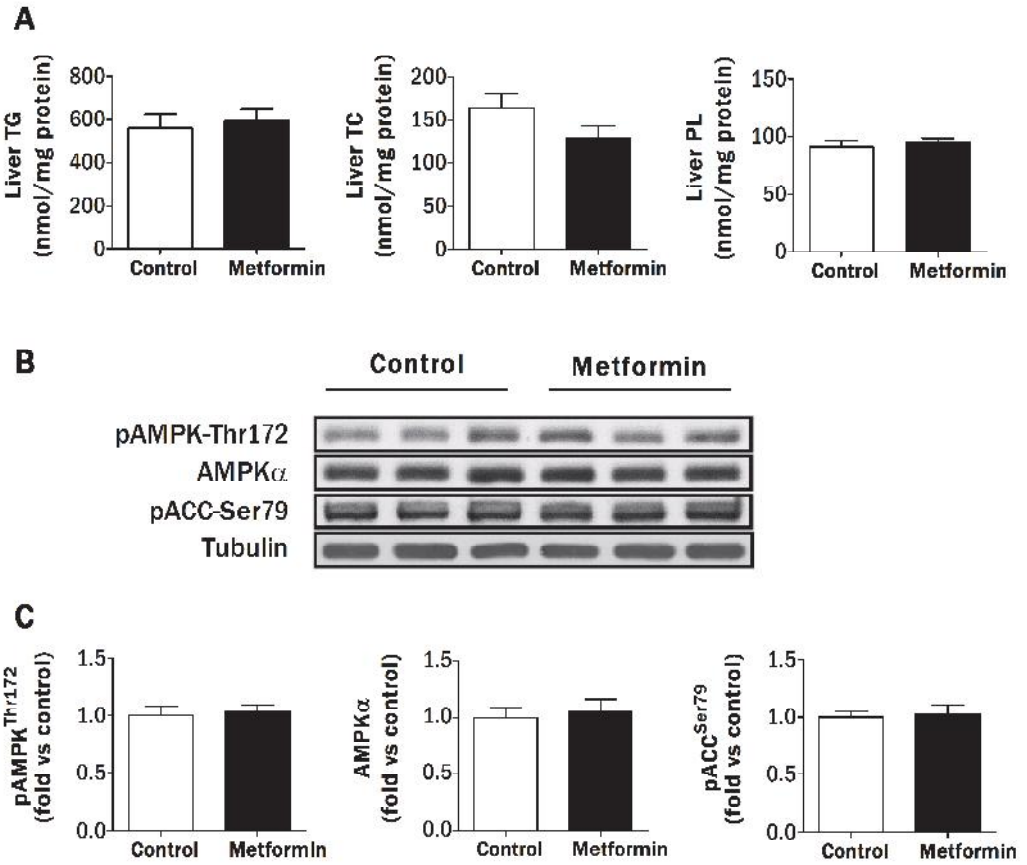

Supplemental Figure 2. Effect of metformin on hepatic lipid composition and AMPK signalling. Livers from 4 h-fasted mice were collected after 4 weeks of treatment with (black bars) or without metformin (control, open bars) and immediately snap-frozen in liquid nitrogen. Hepatic TG, TC and PL content were measured after lipid extraction (A). The phosphorylation state of Thr172-AMPK and Ser79-ACC, and AMPKα protein expression were assessed on tissue lysate by Western blot (B), followed by densitometric quantification (C). Tubulin expression was used as internal housekeeping protein. Data are means ± SEM (n=5-8 per group).

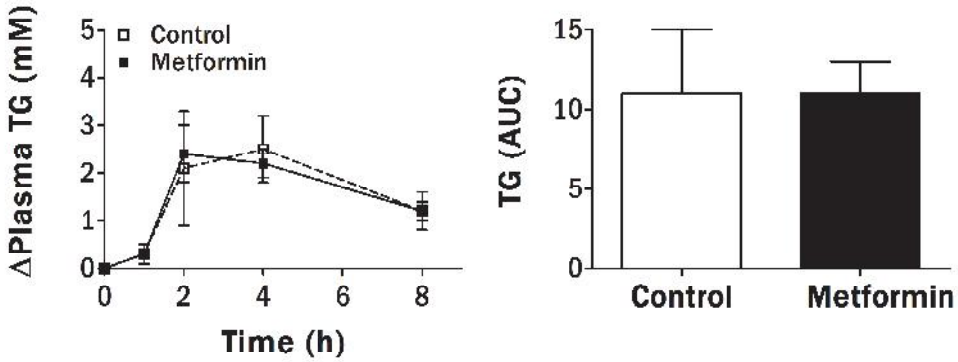

Supplemental Figure 3. Effect of metformin on postprandial TG response. Overnight-fasted control (open squares) and metformin-treated (black squares) mice were given an intragastric bolus of 200 µl of olive oil. Blood samples were drawn at 0, 2, 4, and 8 h. TG concentrations were determined in plasma and corrected for their respective values at time 0. Values are means ± SEM (n=9-10/group).